Critical Evaluation and Optimization of the Thermodynamic Properties and Phase Diagrams of the CrO-Cr2O3-SiO2 and CrO-Cr2O3-SiO2-Al2O3 Systems

S. Degterov and A.D. Pelton
Centre de Recherche en Calcul Thermochimique
École Polytechnique de Montréal
P.O. Box 6079, Station "Downtown"
Montreal, Quebec, Canada, H3C 3A7

(Submitted May 28, 1996; in revised form September 9, 1996)

Available thermodynamic and phase diagram data have been critically assessed for all phases in the CrO-Cr_2O_3-SiO_2 and CrO-Cr_2O_3-SiO_2-Al_2O_3 systems from 298 K to above the liquidus temperatures and for oxygen partial pressures ranging from equilibrium with metallic Cr to equilibrium with air. All reliable data have been simultaneously optimized to obtain one set of model equations for the Gibbs energy of the liquid slag and all solid phases as functions of composition and temperature. The modified quasi-chemical model was used for the slag. The models permit phase equilibria to be calculated for regions of composition, temperature, and oxygen potential where data are not available.

1. Introduction

This is the second in a series of three articles on the inclusion of chrome oxides in a database of optimized thermodynamic properties of oxide systems. In the first article (Ref 1), the methodology is described, the modified quasi-chemical model, which is used for the molten slag phase, is outlined, and optimizations are performed for the CrO-Cr_2O_3, CrO-Cr_2O_3-Al_2O_3, and CrO-Cr_2O_3-CaO systems. The third article of the series (Ref 2) treats the optimization of the CrO-Cr_2O_3-SiO_2-CaO system.

Evaluated and optimized thermodynamic properties of CrO (liquid), Cr_2O_3, and Cr_3O_4 are tabulated in the first article (Ref 1), while those of Al_2O_3, SiO_2, and $Al_6Si_2O_{13}$ (mullite) are given in an earlier publication (Ref 3) on the optimization of the Al_2O_3-SiO_2 system. A thermodynamic model for the nonstoichiometry of mullite in the Al_2O_3-SiO_2 system is also described (Ref 3), and this model is used in the present analysis. The thermodynamic properties of Al_2O_3-Cr_2O_3 solid solutions are modeled, and optimized equations are given in Ref 1. Optimized parameters of the modified quasi-chemical model for the CrO-Cr_2O_3-Al_2O_3 system are given in Ref 1, and those for the Al_2O_3-SiO_2 system are in Ref 3.

2. The CrO-Cr2O3-SiO2 System

The calculated optimized phase diagrams for the system in equilibrium with metallic Cr and at various constant oxygen partial pressures are shown in Fig. 1 and 2(a to g), respectively. Figure 1 is a projection of phase equilibria in the Cr-Si-O system through the Cr-corner to the CrO-SiO_2 join. That is, if CrO and SiO_2 are mixed in a proportion given by a point on this axis, and are equilibrated with an excess of Cr, then the equilibrium phase assemblage can be read from the diagram. The

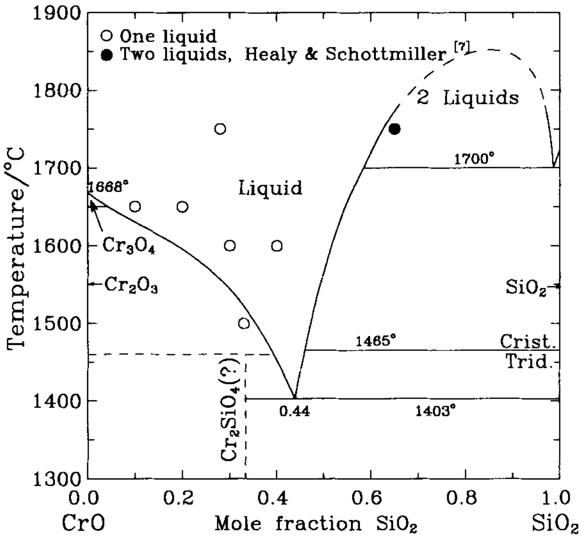

Fig. 1 Calculated CrO-Cr_2O_3-SiO_2 phase diagram in equilibrium with Cr.

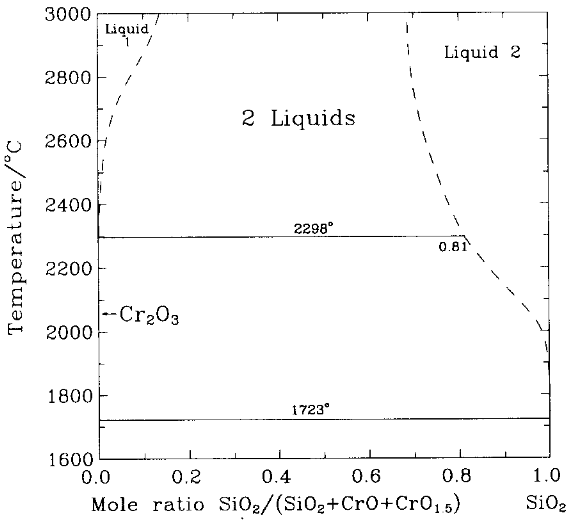

Fig. 2(a) Calculated $CrO-Cr_2O_3-SiO_2$ phase diagram in air.

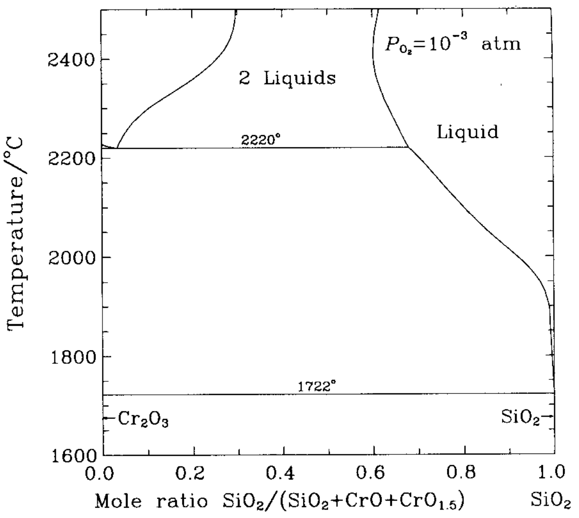

Fig. 2(b) Calculated $CrO-Cr_2O_3-SiO_2$ phase diagram at P_{O_2} = 10^{-3} atm.

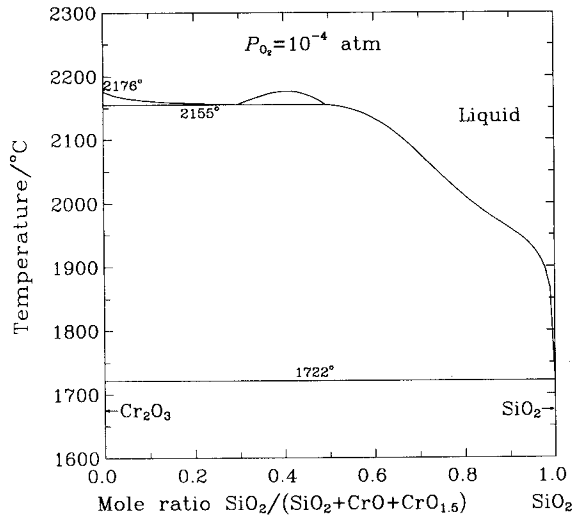

Fig. 2(c) Calculated $CrO-Cr_2O_3-SiO_2$ phase diagram at P_{O_2} = 10^{-4} atm.

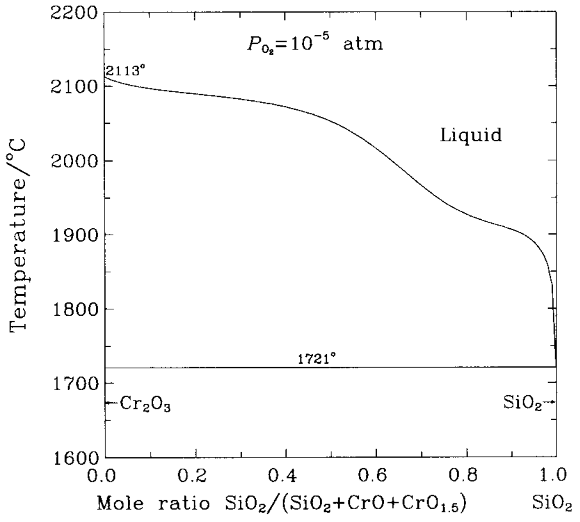

Fig. 2(d) Calculated $CrO-Cr_2O_3-SiO_2$ phase diagram at P_{O_2} = 10^{-5} atm.

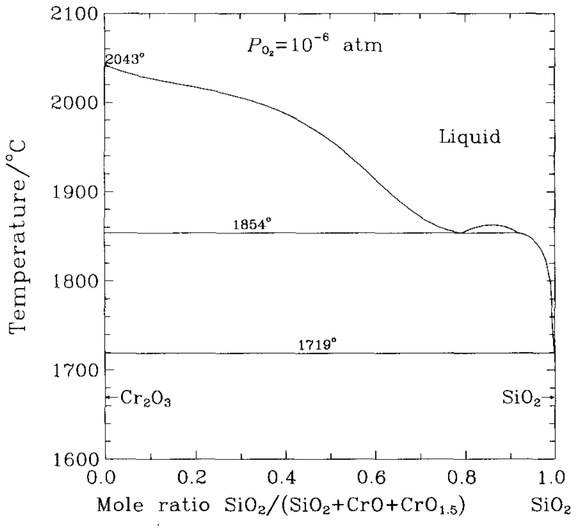

Fig. 2(e) Calculated CrO-Cr_2O_3-SiO_2 phase diagram at P_{O_2} = 10^{-6} atm.

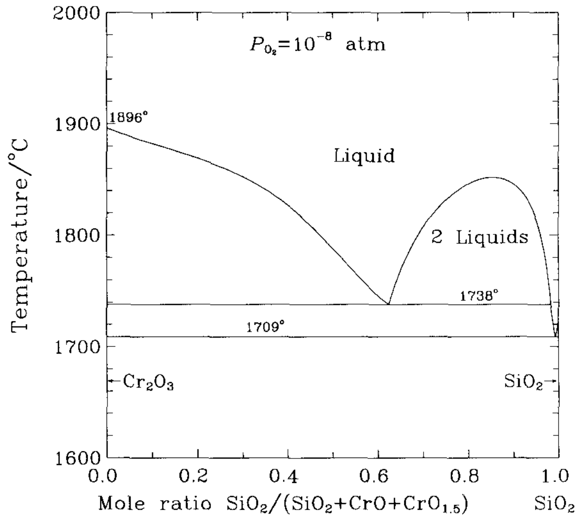

Fig. 2(f) Calculated CrO-Cr_2O_3-SiO_2 phase diagram at P_{O_2} = 10^{-8} atm.

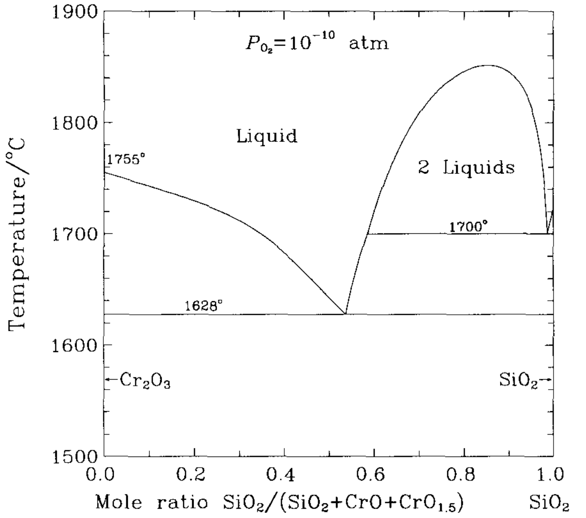

Fig. 2(g) Calculated CrO-Cr_2O_3-SiO_2 phase diagram at P_{O_2} = 10^{-10} atm.

calculated Cr^{3+} content of the liquid in equilibrium with Cr varies from approximately 7% of total Cr at low SiO_2 content, to about 1% at the eutectic point, and to <1% on the SiO_2-rich side of the eutectic. In Fig. 2, the composition axes are $n_{Si}/(n_{Si} + n_{Cr^{2+}} + n_{Cr^{3+}})$, where n_i is the number of moles of species i. In Fig. 2(a), in air, the calculated Cr^{3+} content of Liquid 1 in equilibrium at the monotectic temperature of 2298 °C is 96% of total Cr, while that of Liquid 2 is 0.2% of total Cr. As temperature increases, the proportion of Cr^{3+} to Cr^{2+} in the liquids decreases. In the calculations, the liquid was assumed to contain only divalent and trivalent chrome.

The system in air was first examined by Bunting (Ref 4), who fused mixtures of Cr_2O_3 and SiO_2 in an O_2/H_2 flame, followed by quenching, petrography, and XRD. No intermediate compounds were found. The eutectic temperature was indistinguishable from the melting point of pure SiO_2. The melting point of Cr_2O_3 in air was reported as 2143 °C, but was later revised by the same author to 2270 ± 25 °C (Ref 5). The temperature shown in Fig. 2(a) for the melting point of Cr_2O_3 in air is that obtained from analysis of the CrO-Cr_2O_3 system (Ref 1). From Bunting's description of his experiments, as pointed out by Keith (Ref 6), the monotectic temperature is very close to the melting point of Cr_2O_3 in air.

The system was studied at low P_{O_2} by Healy and Schottmiller (Ref 7). Their results for melting experiments involving mixtures of Cr_2O_3, Cr, and SiO_2 held in tungsten crucibles under purified Ar are shown in Fig. 1. Healy and Schottmiller determined the equilibrium H_2/H_2O ratios over various fused mix-

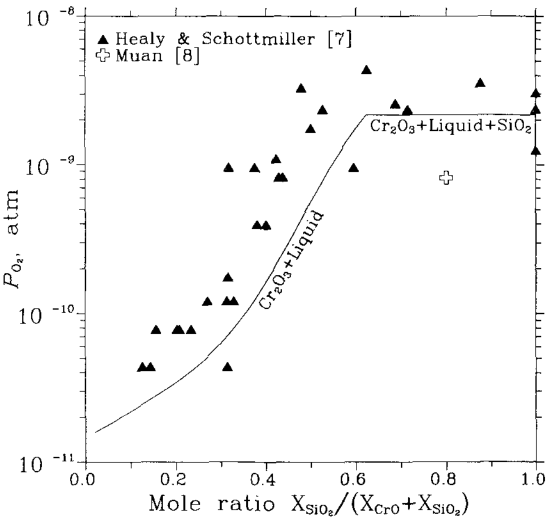

Fig. 3 Calculated equilibrium oxygen pressure in two-phase and three-phase regions of the $CrO-Cr_2O_3-SiO_2$ system at 1700 °C.

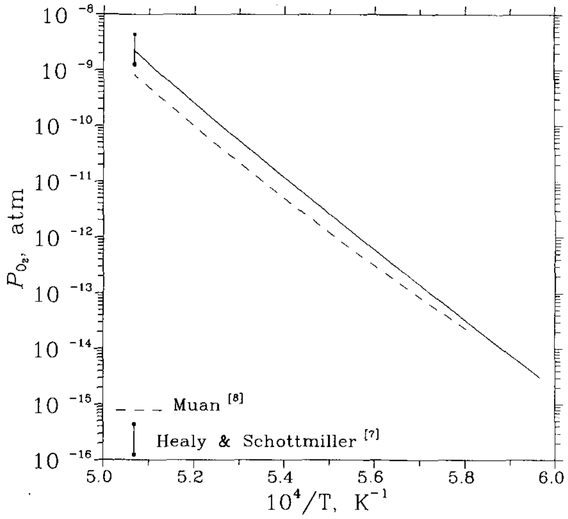

Fig. 4 Calculated equilibrium oxygen pressure for three-phase ($Cr_2O_3 + SiO_2 + L$) equilibrium in the $CrO-Cr_2O_3-SiO_2$ system.

Table 1 Calculated Invariant Points Involving the Liquid in the $Cr-Cr_2O_3-SiO_2$ System

Reaction	Temperature, °C	P_{O_2},atm	Liquid composition, mol %		
			CrO	Cr_2O_3	SiO_2
$L + SiO_2 \rightarrow L_2 + Cr_2O_3$....	1701	2.3×10^{-9}	36.6	2.6	60.8
			1.3	~0.0	98.7
$L + SiO_2 \rightarrow L_2 + Cr$..........	1700	6.6×10^{-13}	41.5	~0.0	58.4
			1.4	~0.0	98.6
$L \rightarrow Cr_2O_3 + SiO_2 + Cr$....	1403	3.0×10^{-15}	55.6	0.3	44.1

tures of Cr_2O_3, Cr, and SiO_2 of known overall composition. This permitted them to determine P_{O_2} for the three-phase ($Cr_2O_3 + L + SiO_2$) region and for the two-phase ($Cr_2O_3 + L$) region as a function of composition as shown in Fig. 3. For the calculated curve in Fig. 3, the Cr^{3+} content of the liquids in equilibrium with Cr_2O_3 varies from 2 to 12% of total Cr in the liquid.

The phase diagram in equilibrium with Cr was reported by Muan (Ref 8), although no description whatsoever of the experiments was given. A eutectic at about 1400 °C and about 43 mol% SiO_2 was reported, as well as a monotectic temperature of about 1710 °C. Muan also reported the oxygen partial pressure as a function of temperature for the univariant ($L + Cr_2O_3 + SiO_2$) line, again with no experimental description. His curve is plotted in Fig. 4, and his value at 1700 °C is shown in Fig. 3.

Muan (Ref 8) reported no intermediate compounds. However, Healy and Schottmiller (Ref 7) observed a blue silicate phase at low P_{O_2}, melting at about 1400 to 1500 °C, which they characterized by XRD and whose composition—as determined by chemical analysis—corresponded closely to Cr_2SiO_4. This compound is shown tentatively in Fig. 1.

The data were optimized to yield the following binary quasichemical parameters for the liquid (where the notation of Ref 1 is used). No ternary parameters were required.

$$\omega^{07}_{CrO-SiO_2} = 754\ 823\ Y^{7}_{SiO_2}\ \text{J/mol} \qquad \text{(Eq 1)}$$

$$\eta^{07}_{CrO-SiO_2} = 325.372\ Y^{7}_{SiO_2}\ \text{J/mol} \cdot \text{K} \qquad \text{(Eq 2)}$$

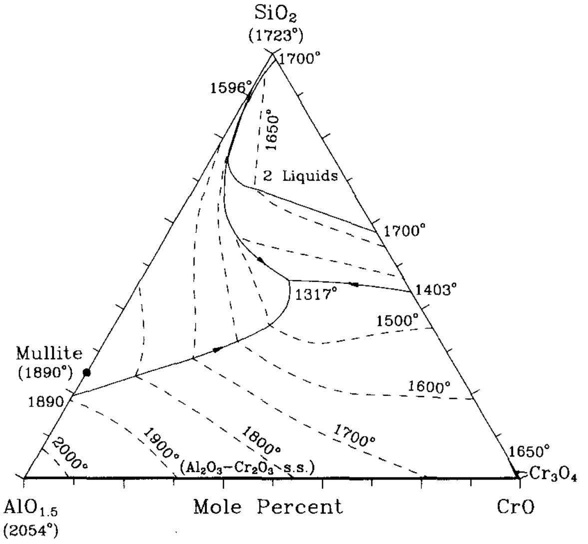

Fig. 5 Calculated $CrO-Cr_2O_3-SiO_2-Al_2O_3$ liquidus in equilibrium with Cr (*T* in °C).

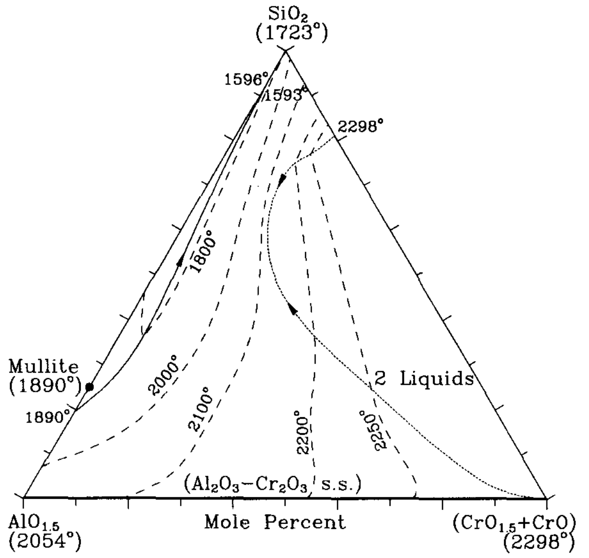

Fig. 6 Calculated $CrO-Cr_2O_3-SiO_2-Al_2O_3$ liquidus in air (*T* in °C).

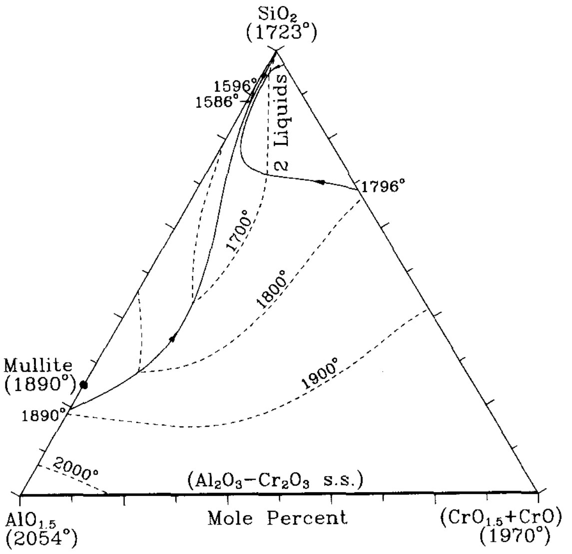

Fig. 7 Calculated $CrO-Cr_2O_3-SiO_2-Al_2O_3$ liquidus at $P_{O_2} = 10^{-7}$ atm.

$$\omega^{00}_{CrO_{1.5}-SiO_2} = 167\,360 \text{ J/mol} \qquad \text{(Eq 3)}$$

The seventh power of Y_{SiO_2} in Eq 1 and 2 was chosen so as to reproduce the miscibility gap in Fig. 1. The use of this power has been found to give good results for several similar AO-SiO_2 systems where AO is a basic oxide.

Calculated invariant points involving the liquid phase are listed in Table 1.

The unusual shape of the calculated miscibility gap in Fig. 2(b) can be attributed to the fact that the Cr^{3+}/Cr^{2+} ratio changes with temperature at constant P_{O_2}. On the other hand, no data are available at these high temperatures, so the predictions are only tentative at these temperatures.

3. The $CrO-Cr_2O_3-SiO_2-Al_2O_3$ System

The calculated optimized liquidus projection for the system in equilibrium with metallic Cr, with air, and at $P_{O_2} = 10^{-7}$ atm are shown in Fig. 5 to 7, respectively. Figure 8 shows a calculated isothermal section at 1700 °C. Figure 5 is a projection of liquidus phase equilibria in the Cr-Si-Al-O tetrahedron through the Cr-corner onto the $CrO-AlO_{1.5}-SiO_2$ plane. That is, if CrO, $AlO_{1.5}$, and SiO_2 are mixed in a proportion given by a point on this diagram and are equilibrated with excess Cr, then the equilibrium phase assemblage can be read from the diagram. The calculated Cr^{3+} content of the liquid in equilibrium with Cr at liquidus temperatures varies from a maximum of about 9% of total Cr at very low SiO_2 content to <1% of total Cr at high SiO_2 contents. In Fig. 6 and 7, the composition axes are to be interpreted as $X_{SiO_2} = n_{Si}/n_{TOT}$, $X_{AlO_{1.5}} = n_{Al}/n_{TOT}$, and $X_{(CrO_{1.5}+CrO)} = (n_{Cr^{2+}} + n_{Cr^{3+}})/n_{TOT}$, where n_i is the number of moles of species i and $n_{TOT} = (n_{Si} + n_{Al} + n_{Cr^{2+}} + n_{Cr^{3+}})$. It is assumed in the calculations that only divalent and trivalent Cr are found in the liquid phase.

A liquidus surface for the system in equilibrium with Cr was reported by Muan (Ref 8), but no description whatsoever of the experiments was given. Muan's diagram is quite similar to the calculated diagram in Fig. 5, with a eutectic between 1300 and 1350 °C at the same composition as in Fig. 5. Muan also reported the temperature-P_{O_2} curve for the four-phase equilibrium (mullite + SiO_2 + $(Al,Cr)_2O_3$ + L). His results are shown in Fig. 9. Again, no experimental description was given.

The system was studied in air by Roeder et al. (Ref 9). Because temperatures were limited to the range 1580 to 1880 °C, only equilibrium liquids at low chrome contents were studied. These authors report a long narrow primary crystallization region for mullite and a very small field for SiO_2. The ternary eutectic was reported to lie at 1580 °C at less than 1 mol% Cr_2O_3. Results of quenching experiments by Roeder et al. at 1700 °C are shown in Fig. 8. Apart from one experimental point, the calculations and experimental results are in agreement. Roeder et al. (Ref 9) also estimated the compositions of the Al_2O_3-Cr_2O_3 solid solutions in equilibrium with the liquid by means of x-ray determinations of lattice parameters and a calibration curve. These results were not always in good agreement with the results of the quenching experiments with regard to the composition of the Al_2O_3-Cr_2O_3 solution in the three-phase (mullite + L + Al_2O_3-Cr_2O_3) region. At 1700 °C their x-ray results give this corner of the three-phase triangle at approximately 43 wt.% Cr_2O_3-57 wt.% Al_2O_3. The authors reported much difficulty in attaining equilibrium. Ford and Rees (Ref 10) studied the mullite-Cr_2O_3 join at 1600 °C in air by quenching followed by XRD and petrography. The Cr_2O_3-rich boundary of the three-phase (mullite + L + $(Al,Cr)_2O_3$) region at 1600 °C was observed at 47 wt.% Cr_2O_3, in reasonable agreement with the calculated value of 52 wt.% Cr_2O_3.

Ford and Rees (Ref 10) reported a solubility of 8 wt.% Cr_2O_3 in mullite at 1600 °C. By studying changes in lattice parameters, Murthy and Hummel (Ref 11) reported dissolution of 3, 6, and 10 wt.% Cr_2O_3 in mullite at 1700, 1600, and 1400 °C, respectively. Roeder et al. (Ref 9), on the other hand, were unable to obtain single-phase mullite containing Cr_2O_3. In the optimization, mullite was assumed to dissolve no chrome.

The system was optimized with the following ternary quasichemical parameter for the liquid phase (employing the notation of Ref 1):

$$\omega^{001}_{CrO,\,SiO_2(AlO_{1.5})} = -29\,288 \text{ J/mol} \qquad \text{(Eq 4)}$$

All available phase equilibrium data are reproduced within experimental error limits, including the T-P_{O_2} curve for the four-

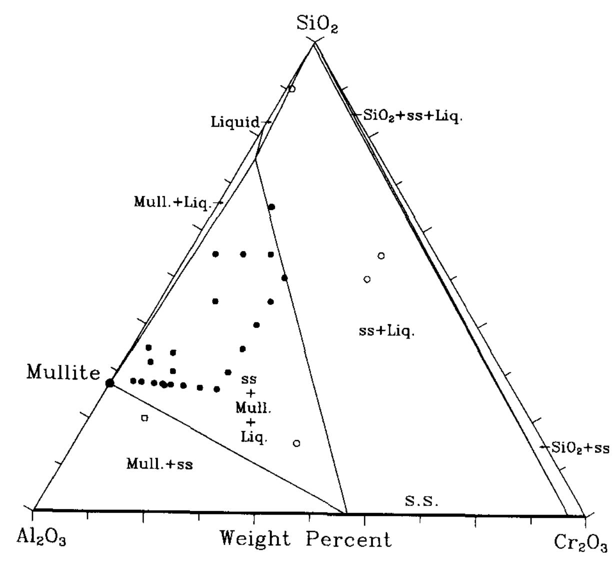

Fig. 8 Calculated section of the Al_2O_3-Cr_2O_3-SiO_2 phase diagram in air at 1700 °C. Points are from quenching experiments of Roeder et al. (Ref 9): ●, mullite + L + Al_2O_3-Cr_2O_3 solid solution; ○, L + Al_2O_3-Cr_2O_3 solid solution; □, mullite + Al_2O_3-Cr_2O_3 solid solution.

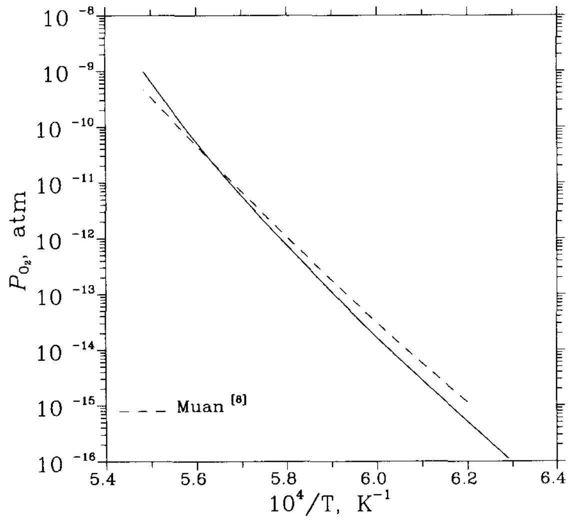

Fig. 9 Calculated oxygen partial pressure for the four-phase equilibrium $(Al,Cr)_2O_3$ + SiO_2 + mullite + L.

phase equilibrium in Fig. 9. The eutectic in air in Fig. 6 is calculated to lie at 1593 °C at very low chrome content. The probable maximum inaccuracy in the calculated liquidus is estimated as ±50 °C.

Acknowledgments

This work was supported by the Natural Sciences and Engineering Research Council of Canada and by the Alberta Research Council.

Cited References

1. S. Degterov and A.D. Pelton, *J. Phase Equilibria, 17*(6), 476-487 (1996).
2. S. Degterov and A.D. Pelton, *Metall. Trans.*, in press.
3. G. Eriksson and A.D. Pelton, *Metall. Trans. B, 24.*, 807-816 (1993).
4. E.N. Bunting, *Bur. Std. J. Res., 5*, 325-327 (1930).
5. E.N. Bunting, *Bur. Std. J. Res., 6*, 947-949 (1931).
6. M.L. Keith, *J. Am. Ceram. Soc., 37*, 490-496 (1954).
7. G.W. Healy and J.C. Schottmiller, *TMS-AIME, 230*, 420-425 (1964).
8. A. Muan, *High Temp.-High Press., 14*, 653-660 (1982).
9. P.L. Roeder, F.P. Glasser, and E.F. Osborn, *J. Am. Ceram. Soc., 51*, 585-594 (1968).
10. W.F. Ford and W.J. Rees, *Trans. Brit. Ceram. Soc., 45*, 125-136 (1946).
11. M.K. Murthy and F.A. Hummel, *J. Am. Ceram. Soc., 43*, 267-273 (1960).